Proceedings of the Tenth EGS4 Users' Meeting in Japan, KEK Proceedings 2002-18, p.74-83

THE VARIATIONS OF MEAN MASS ENERGY ABSORPTION COEFFICIENT RATIOS IN WATER PHANTOMS DURING X-RAY CT SCANNING

S. Miyajima
Graduate School of Medicine, Course of Health Sciences, Osaka University
1-7 Yamadaoka, Suita, Osaka, 565-0871, Japan
satoshi@sahs.med.osaka-u.ac.jp

Abstract

Mean mass energy absorption coefficient ratios were computed from x-ray spectra in water phantoms during x-ray computed tomography (CT) scanning. The x-ray spectra were calculated with LSCAT (EGS4 for low energy x-rays). The calibration factors in dosimetry, which relate the output of detectors to the absorbed dose in water, were obtained from the ratios. The errors in patient dosimetry in CT scanning, related to the calibration procedure, were evaluated using the calculated calibration factors.

1 Introduction

Detector response is based on the interaction of x-rays with detector materials: the output of detectors arises from the absorbed dose attributed to the interaction. Since mass x-ray absorption coefficients μ_{en}/ρ have a wide variation in the range of diagnostic radiology (Fig. 1), the detector response may depend heavily on x-ray energy in the diagnostic energy range. To estimate the energy-dependence of the response, x-ray spectra at the point of interest are essential.

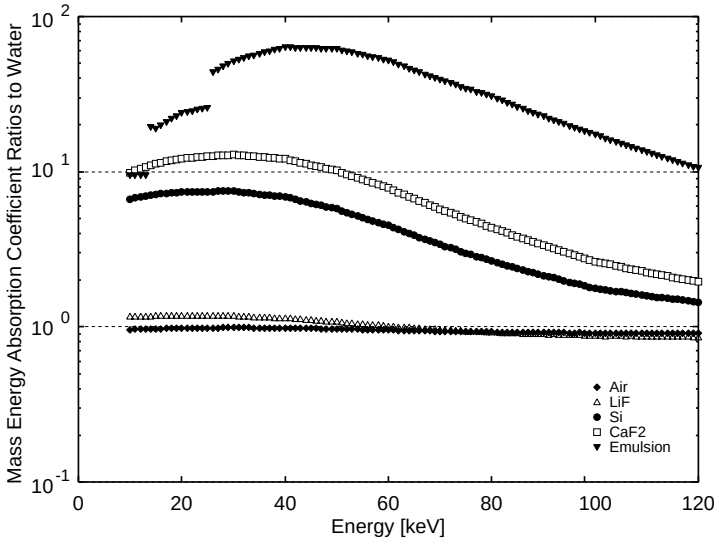

Figure 1: The ratios of mass energy absorption coefficients of various detector materials to those of water. The coefficients were obtained from the data published by Hubbell [1]

In patient dosimetry, detectors are placed in phantoms which simulate an human body. X-ray spectra in phantoms, however, are rarely known because it is difficult to measure them. Hence, some assumptions have been made in the calibration of detectors.

The calibration procedure which is usually employed is as follows:

(1) irradiate both the reference detector and detectors that will be placed in phantoms simultaneously with the incident x-rays. An ionization chamber is usually employed as the reference detector because air has almost the same x-ray absorption property as water. Note that soft-tissue is almost water-equivalent,

(2) calculate the absorbed dose in water from exposure obtained with an ionization chamber. The ratio of mass energy absorption coefficient of water to air at the effective energy of incident x-rays is used to calculate the absorbed dose in water,

(3) obtain the calibration factor, i.e. the ratio of detector readings to the absorbed dose in water calculated in (2). The factor will be used to convert the reading to the absorbed dose in water.

In this calibration procedure, x-ray spectra in phantoms are assumed to be the same as those of incident x-rays. Moreover, x-rays are regarded as monoenergetic: the mass energy absorption coefficient at the effective energy of incident x-rays is utilized in the procedure. This means that the spectral distribution of x-rays is neglected.

Our calculation with the EGS4 code, however, revealed that x-ray spectra in phantoms were quite different from those of incident x-rays [2]. Besides, the mass energy absorption coefficients vary significantly in the diagnostic energy range (Fig.1). Hence, the assumptions made in the calibration procedure may cause under- or over-estimation in patient dose.

In this article, the errors in patient dose related to the calibration procedure are estimated. The mean mass energy absorption coefficient ratios $\overline{(\mu_{en}/\rho)}_{water}^{material}$, which are the ratios of the absorbed dose in detector materials to water, are calculated. The calibration factors are obtained from the ratios, and compared with those which are obtained with the usual calibration procedure.

2 Materials and Methods

2.1 Calculation of x-ray spectra in water phantoms

The x-ray transport in water phantoms was simulated with the Monte Carlo method. The details of the calculations are in our previous paper [2].

The model in the calculation is in Figure 2. The cylindrical water phantoms were 60 cm in length and 16 cm (head phantom) or 32 cm (body phantom) in diameter. An x-ray source was rotated through 360 degrees, and emitted fan beams. X-rays from the source were the ones generated with the tube voltage of 120 kV. The effective energy of the incident x-rays ranged from 40 to 70 keV. The energy of x-rays which passed across the volumes of 1 cm long and 1 cmϕ in the phantoms was scored.

The code LSCAT [3] (EGS4 for low energy photons) was employed in the calculation. The photoelectric effect, the Rayleigh scattering and the Compton scattering with bound electrons were taken into account. The cut-off energy for x-rays was 5.0 keV. The electron path was neglected, i.e. secondary electrons were absorbed where they are generated.

2.2 Calculation of mean mass energy absorption coefficient ratios

The mean mass energy absorption coefficient is calculated using Monte Carlo generated x-ray spectra in the water phantoms:

$$\overline{\mu_{en}/\rho} = \frac{\int (\mu_{en}(E)/\rho) E\phi(E) dE}{\int E\phi(E) dE} \tag{1}$$

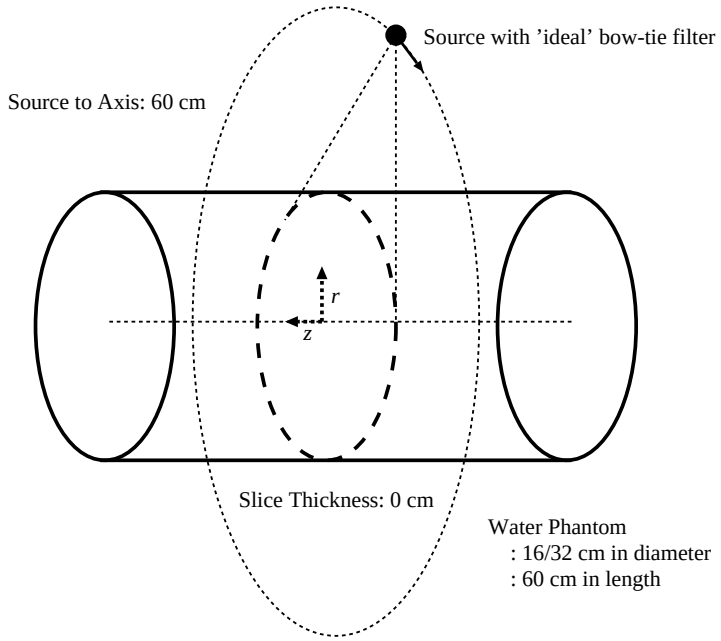

Figure 2: The model in the calculation of x-ray spectra in the water phantom. z is the distance from the scanned volume and r is that from the phantom axis.

where $\overline{\mu_{en}/\rho}$ is the mean mass energy absorption coefficient, $\mu_{en}(E)/\rho$ is the mass energy absorption coefficient at energy E, and $\phi(E)$ is fluence at energy E, i.e. the number of photons with energy E.

It should be noted that the numerator of Equation (1) is the absorbed dose in materials in the energy fluence $E\phi(E)$, and the dominator is the energy fluence. Therefore, the mean mass energy absorption coefficient is the absorbed dose per unit energy fluence.

The ratio of the mean mass energy absorption coefficients of two media a and b is defined as [4][5]

$$\overline{(\mu_{en}/\rho)}^{a}_{b}(z,r) = \frac{\int (\mu_{en}(E)/\rho)_a E\phi(E,z,r)dE}{\int (\mu_{en}(E)/\rho)_b E\phi(E,z,r)dE} \tag{2}$$

where $\overline{(\mu_{en}/\rho)}^{b}_{a}(z,r)$ is the mean mass energy absorption coefficient ratio at the position (z,r) in the phantoms, and $\phi(E,z,r)$ is fluence at (z,r) and at energy E.

$\overline{(\mu_{en}/\rho)}^{b}_{a}(z,r)$ is the ratio of the absorbed dose in material a to that in material b in the same energy fluence. The ratios of the absorbed dose in detector materials to that in water, i.e. $\overline{(\mu_{en}/\rho)}^{material}_{water}(z,r)$, were calculated in this study.

2.3 Relation between calibration factors and mean mass energy absorption coefficient ratios

The calibration factors, which relate detector output to the absorbed dose in water, were calculated. The factors are the reciprocal of $\overline{(\mu_{en}/\rho)}^{material}_{water}(z,r)$. The factors were compared with those obtained with the usual method, which is explained in the introduction. Note that the latter does not take both the variations of x-ray spectra in phantoms and those of the mass energy absorption coefficients into account.

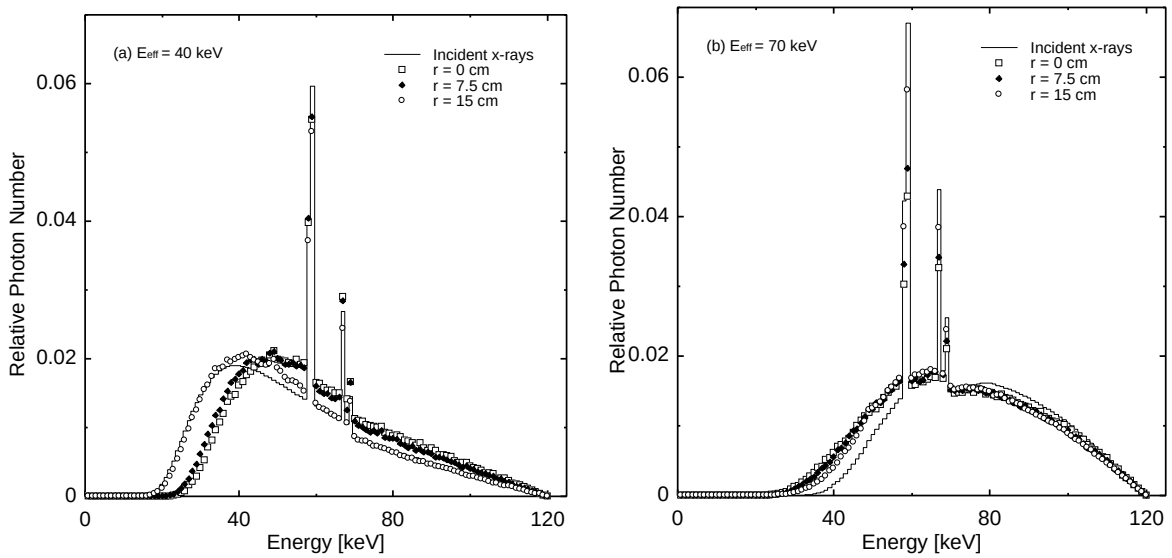

Figure 3: The variations of x-ray spectra in the scanned volume of the water phantom of 32 cmϕ. The effective energy of the incident x-rays are (a) 40 keV and (b) 70 keV. The parameter r is the distance from the phantom axis. All the spectra are normalized to unit area.

3 Results

3.1 Variations of x-ray spectra in water phantoms

Figure 3(a) and (b) show that the variations of x-ray spectra in the scanned volume of the water phantoms of 32 cmϕ. The spectra in the phantoms are not the same as the incident spectra. In addition, the spectra are dependent on the positions in the scanned volume of the phantoms. It should be noted that x-rays in the phantoms are harder than the incident x-rays with the effective energy of 40 keV, while softer than that of 70 keV.

Figure 4(a) and (b) show that the variations of x-ray spectra in the axis of the water phantom of 32 cmϕ. The spectra in the phantom axis are far different from those of incident x-rays. Furthermore, the spectra depend on the positions in the phantoms. Note that the spectra at at $z = 0$ cm is quite different from the others because those at $z = 0$ contains incident x-rays, while the others does not.

The same tendency was observed with the phantom of 16 cmϕ in both the scanned volume and the axis of the phantoms.

3.2 Variations of mean mass energy absorption coefficient ratios and calibration factors

Figure 5 shows that the example of (a) $\overline{(\mu_{en}/\rho)}_{water}^{material}(z,r)$ calculated from x-ray spectra in the phantoms, using Equation (2), and (b) calibration factors obtained from $\overline{(\mu_{en}/\rho)}_{water}^{material}(z,r)$. Note that the calibration factors are the reciprocal of $\overline{(\mu_{en}/\rho)}_{water}^{material}(z,r)$.

3.3 Errors in calibration factors

The calibration factors $CF_{in-phantom}$ were obtained from $\overline{(\mu_{en}/\rho)}_{water}^{material}(z,r)$, which were calculated from x-ray spectra in the phantoms. They were compared with $CF_{incident}$ calculated using the incident x-rays and the mass energy absorption coefficient ratios at the effective energy of the

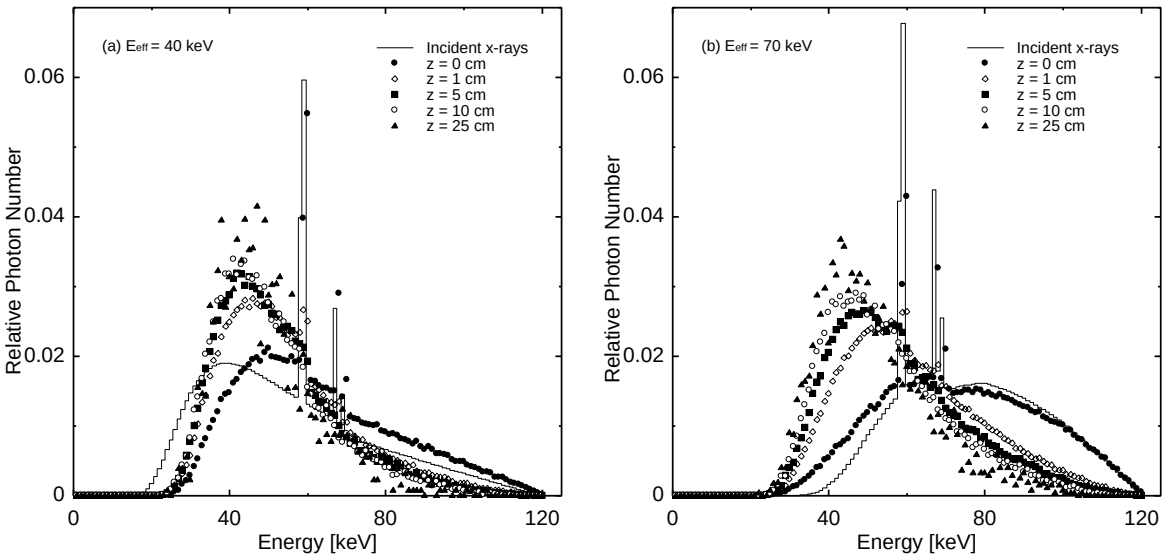

Figure 4: The variations of x-ray spectra in the axis of the water phantom of 32 cmϕ. The effective energy of the incident x-rays are (a) 40 keV and (b) 70 keV. The parameter z is the distance from the scanned volume. All the spectra are normalized to unit area.

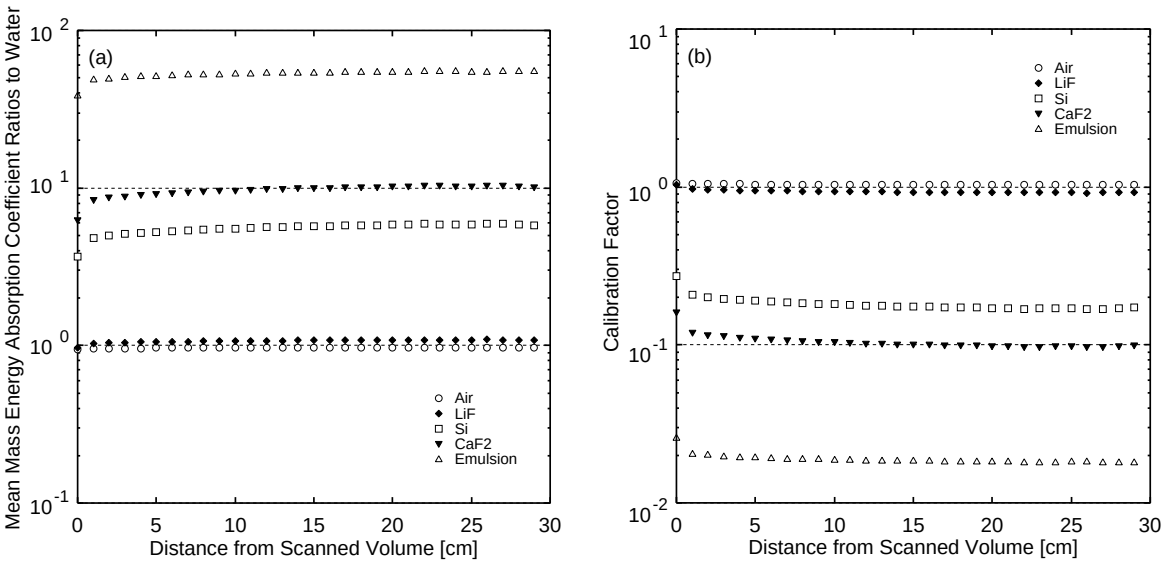

Figure 5: The example of (a) the calculated mean mass energy absorption coefficient ratios with (b) the calibration factors on the axis of the phantoms. The effective energy of incident x-rays is 70 keV, and the phantom diameter is 32 cmϕ.

Table 1: The calibration factors obtained with the incident x-rays. The factors were the ratios of absorbed dose in each detector materials to that in water, irradiated with the incident x-rays. The absorbed dose in water was calculated from that in air, using the ratios of the mass energy absorption coefficients of air and water at the effective energy of the incident x-rays. The absorbed dose in each detector material was calculated using the incident x-ray spectra and mass energy absorption coefficients.

E_{eff}	Air	LiF	Si	CaF_2	Emulsion
40 keV	1.01668	0.91335	0.17421	0.10121	0.02074
50 keV	1.03050	0.95639	0.20517	0.11882	0.02092
60 keV	1.04900	1.00417	0.24898	0.14533	0.02342
70 keV	1.06494	1.04739	0.30516	0.18147	0.02789

incident x-rays (Table 1). The errors in the calibration factors, i.e. the ratios of $CF_{incident}$ to $CF_{in-phantom}$, were calculated. The results for the phantom of 32 cmϕ are shown in Figure 6 and 7. The same tendency was observed with the phantom of 16 cmϕ.

4 Discussion

4.1 Variations of x-ray spectra in water phantoms

Figure 3 and 4 show that x-ray spectra in the phantoms are quite different from those of the incident x-rays. This implies that the assumption in calibration procedure (see the introduction) contains a critical problem.

The variations of x-ray spectra in water phantoms result from the photoelectric effect and the Compton scattering, which occur in phantoms. Though the Rayleigh scattering happens to some extent in phantoms, the attribution to the variations is minor because x-ray energy does not change after the Rayleigh scattering.

While the photoelectric effect is predominant in water below 30 keV, the Compton scattering is dominant above 30 keV. The spectral variations in the phantoms result from these two effects, i.e. the beam-hardening effects due to the photoelectric effect and the beam-softening effect due to the Compton scattering [2]. Note that the spectral shape at a long distance from the scanned volume is similar regardless of incident x-ray spectra (Fig. 4).

4.2 Errors in calibration factors

The effects of the spectral variations on the errors in the calibration factors are shown in Figure 6 and 7.

The data clearly show that the errors depend on the quality of incident x-rays and the positions in the phantoms. On the whole, the errors are more obvious in higher atomic number materials.

In the axis, the errors are larger in the higher effective energy of incident x-rays. It should be noted that the values in the scanned volume at the axis of the phantoms ($z = 0$) are quite different from the others in the axis (Fig. 7). This discrepancy reflects the spectral difference in the axis (Fig. 4).

In some cases in the scanned volume, the values are less than unity (Fig. 6): this means that the absorbed dose will be underestimated. The underestimation of the patient dose is problematic from the viewpoint of radiation protection.

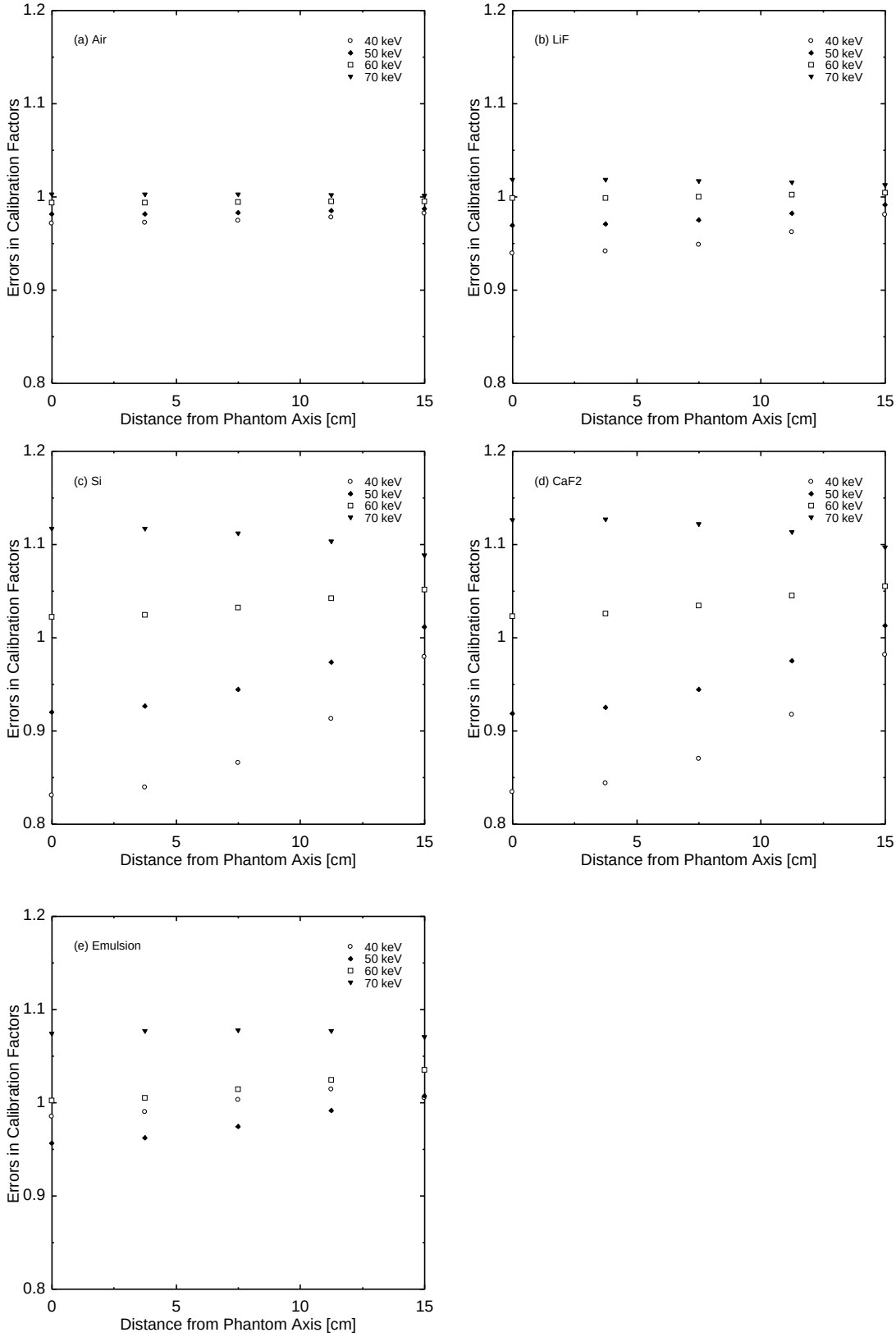

Figure 6: The errors in calibration factors in the scanned volume of the water phantom of 32 cmϕ: (a) air, (b) LiF, (c) Si, (d) CaF_2, and (e) photographic emulsion (KODAK type AA). The parameters are the effective energy of incident x-rays.

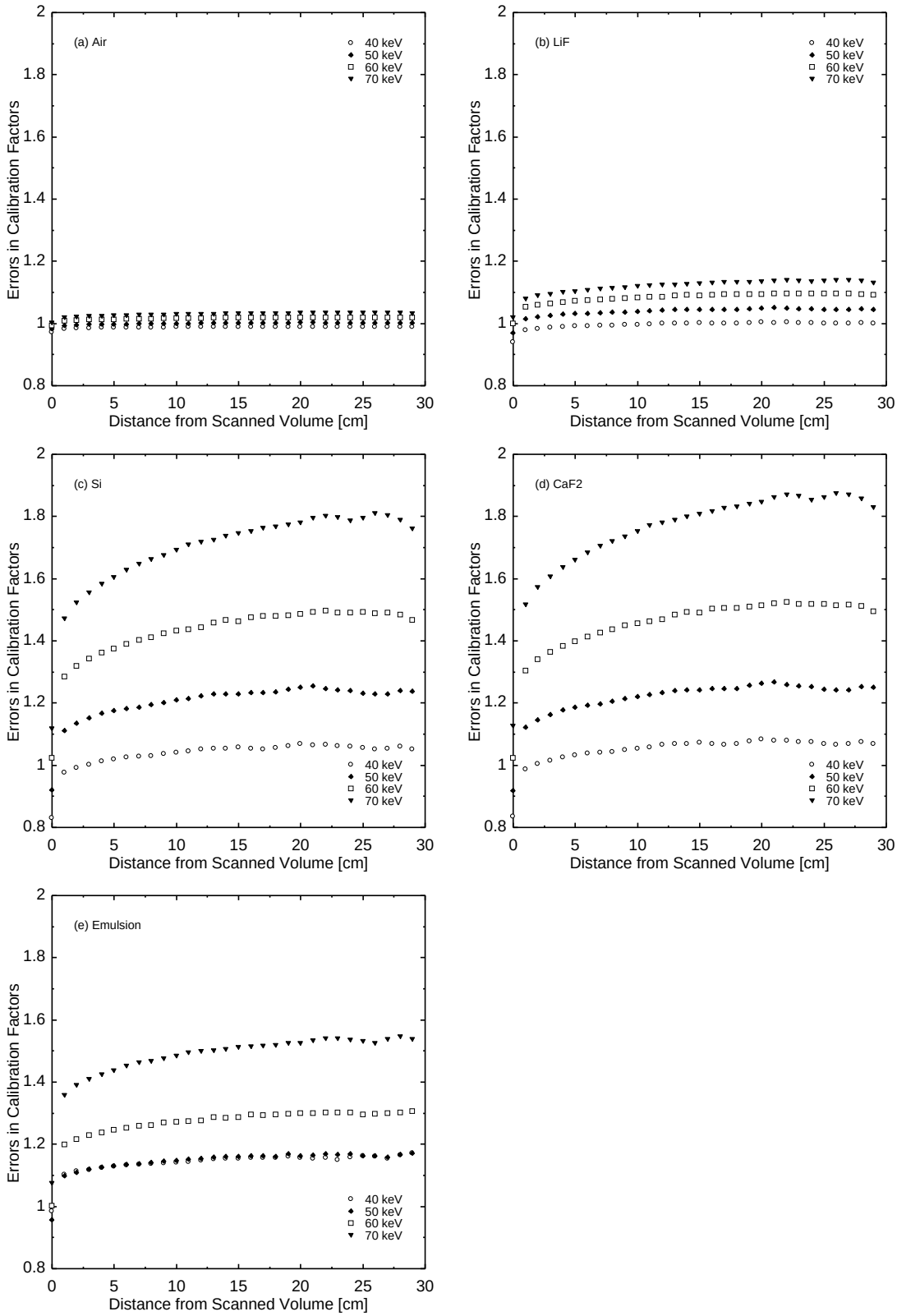

Figure 7: The errors in calibration factors in the axis of the water phantom of 32 cmϕ: (a) air, (b) LiF, (c) Si, (d) CaF_2, and (e) photographic emulsion (KODAK type AA). The parameters are the effective energy of incident x-rays.

4.2.1 Air

In air (Z_{eff}: 7.78 [6]), whose effective atomic number is close to that of water (Z_{eff}: 7.51 [6]), the errors will be within $\pm 3.5\%$.

4.2.2 Lithium fluoride

Lithium fluoride (LiF: $Z_{eff} = 8.2$ [7]) will cause small errors in dosimetry, though the detector is referred to as a tissue-equivalent detector. The maximum errors will be around 15%.

4.2.3 Silicon and calcium fluoride

Silicon (Si: atomic number $Z = 14$) and calcium fluoride (CaF_2: $Z_{eff}= 16.3$ [7]) will cause relatively large errors in the axis of the phantoms, especially in case of high effective energy of incident x-rays (Fig. 7). The errors are also large in the scanned volume (Fig. 6).

4.2.4 Photographic emulsion

Photographic emulsion (Z of silver = 47 and Z of bromine = 35) has different characteristics from the others: the factors for the incident x-rays of 40 keV and that of 50 keV is almost the same. This is probably due to the K-edge of Ag and Br (Fig. 1). Photographic emulsion will cause quite large errors in the axis of the phantoms, especially in case of high effective energy of incident x-rays (Fig. 7).

4.3 Practical calibration procedure

The results obtained in this study indicate that the calibration procedure using incident x-rays is not satisfactory, especially when the detectors with high-atomic number materials are employed. The use of water-equivalent detectors are recommended when the results with high precision are needed. It may be practical to calibrate detectors in appropriate phantoms irradiated with incident x-rays [8]. As x-ray spectra in the scanned volume are quite different from the others, the calibration should be done in and outside the scanned volume separately. Some kind of filters which cover detector materials may improve the energy-dependence of detector response when using high-atomic number detectors.

5 Conclusion

The errors in the calibration procedure of patient dosimetry during CT scanning were evaluated using the mass energy absorption coefficient ratios calculated from x-ray spectra in water phantoms. The results indicates the probability of over- and under-estimation of the absorbed dose in water when using detector materials with the effective atomic numbers different from that of water.

References

[1] J. H. Hubbell and S. M. Seltzer, "Tables of x-ray mass attenuation coefficients and mass energy-absorption coefficients 1 keV to 20 MeV for elements Z = 1 to 92 and 48 additional substances of dosimetric interest", *NISTIR* **5632** (1995).

[2] S. Miyajima *et al*, "Variations of x-ray spectra in water phantom during CT scanning: simulation study", *Radiation Detectors and Their Uses*, KEK Proceedings **2002-12**, 164-174 (2002).

[3] Y. Namito and H. Hirayama, "LSCAT: low-energy photon-scattering expansion for the EGS4 code", KEK Internal **2000-4** (2000).

[4] J. R. Cunningham, M. Woo, D. W. O. Rogers and A. F. Bielajew, "The dependence of mass energy absorption coefficient ratios on beam size and depth in a phantom", Med. Phys. **13(4)**, 496-502 (1986).

[5] E. E. Furhang, C-S Chui and M. Lovelock, "Mean mass energy absorption coefficient ratios for megavoltage x-ray beams", Med. Phys. **22(5)**, 525-530 (1995).

[6] H. E. Johns and J. R. Cunningham, "The physics of radiology (4th ed.)", *Springfield* 142 (1983).

[7] T. N. Pedikal and S. P. Fivozinsky, *NBS handbook* **138** (1982).

[8] K. Nishizawa *et al*, "Determinations of organ doses and effective dose equivalents from computed tomographic examination", Brit. J. Radiol. **64**, 20-28 (1991).